Solid State Polymerization of Poly(ethylene Terephthalate): Kinetic and Property Parameters

S. A. JABARIN and E. A. LOFGREN, *Owens-Illinois, Inc., Toledo, Ohio 43666*

Synopsis

The kinetics of solid state polymerization of poly(ethylene terephthalate) (PET) have been investigated at a variety of conditions. Equations have been developed to describe the relationships of time, temperature, and final molecular weight for PET precursors prepared from specified catalyst and monomer systems. These studies show effects of: time and temperature of solid stating, moisture concentration, oxygen exposure, and nitrogen purge flow rate. Measurements of inherent viscosity, carboxyl end group concentration, melting point, residual acetaldehyde, and acetaldehyde generated during melting are used to monitor molecular weight, purity, and thermal stability of these solid stated resins.

INTRODUCTION

Extensive work has been done to investigate the thermal stability and degradation of PET at temperatures above the melting point. Marshall and Todd[1] studied the effects of oxygen, water, and initial molecular weight of polymers. Goodings[2] measured rate of degradation in terms of polymer viscosity, end group concentration, and analysis of gaseous degradation products. His work was concerned mainly with polycondensation and degradation at 285°C. Kardash et al.[3] worked with model compounds and used weight loss to monitor polymer stability.

The effects of catalyst and stabilizer systems upon polymerization and degradation of PET have also been investigated. Tomita[4] determined rate parameters for propagation and thermal degradation for polycondensation at 283°C using various catalysts. He correlated stability constants of dibenzoyl methane complexes of corresponding metal species with propagation and degradation values, to forecast the catalytic activity of metal compounds. Fontana[5] determined third-order rate constants and activation energies for transesterification reactions catalyzed by lead, zinc, and calcium salts. Chang et al.[6] studied the affects of stabilizers on the preparation of PET, with emphasis on the properties of samples made by the TPA process. Changes in intrinsic viscosity, thermal stability, ethylene glycol, and carboxyl contents were evaluated. The concentration and nature of stabilizers was found to be critical. Zimmermann and co-workers[7-11] have published extensively concerning the effects of metal derivatives (used as transesterification and/or polycondensation catalysts) upon the thermal and thermooxidative properties of polymers. Their findings show changes in type and concentration of catalyst, significantly affect rates of polymerization and degradation. In particular,

Journal of Applied Polymer Science, Vol. 32, 5315–5335 (1986)
 CCC 0021-8995/86/065315-21$04.00

they found PET prepared using antimony catalyst systems to be more resistant to thermal and thermooxidative degradation than samples containing manganese, cobalt, or zinc catalysts. They used changes in carboxyl end group concentration, inherent viscosity, and weight loss during heating to investigate the kinetics of PET degradation. They investigated thermooxidative degradation and found that stabilization of the polymer is achieved by blocking the transesterification catalyst, which is believed to be responsible for the thermal instability of PET. Hydrolytic stability was investigated in water at 100°C, showing cleavage of polymer chains to be autocatalytic in nature. Ravens and Ward[12] studied changes in end-group concentration of PET heated in a flow of dry nitrogen and hydrolyzed under saturated water vapor pressure at temperatures between 150 and 220°C. Rate constants for hydrolysis and polymerization were determined. Hydrolysis was found not to be diffusion controlled, since rates of diffusion are much faster than rates of hydrolysis. McMahon et al.[13] studied rates of hydrolysis, oxidation, and thermal degradation as functions of temperature, relative humidity, and film thickness. They found hydrolysis to be a much larger factor in the deterioration of PET than oxidation or thermal degradation at temperatures up to 130°C. In agreement with Ravens and Ward, they found the activation energy for PET hydrolysis to be about 25 kcal/mol.

Our previously reported investigations[14] followed the kinetics of thermal and thermooxidative degradation of PET as a function of melting temperature, residence time, and environment as well as thermal history and drying environment. Activation energies were calculated for degradation in the presence of oxygen and after exposure to oxygen during drying. Results were compared to those obtained for samples dried and melted in oxygen-free environments. PET is generally prepared commercially by continuous melt phase polymerization to the desired molecular weight or by melt phase polymerization to an intermediate molecular weight precursor, followed by solid state polymerization to achieve high molecular weight resins. This work concerns the polymerization and degradation behavior of PET at solid state conditions and the effects of these conditions on resin molecular weight, purity, and thermal stability.

EXPERIMENTAL

Materials and Sample Preparation

Commercial poly(ethylene terephthalate) (PET) precursors, used for these investigations, were supplied by Goodyear, Firestone, and Eastman chemical companies. Major characteristics are shown in Table I.

Before solid state polymerization, precursor samples were vacuum-dried overnight at 110°C in a shallow tray. Moisture concentrations were reduced to less than 0.005% in order to minimize hydrolytic degradation during the initial stages of polymerization. Samples specifically solid stated with high initial moisture concentrations are designated as "wet" and were used to study the effects of moisture upon the solid state kinetics of molecular weight change. In addition to moisture reduction, overnight drying crystallized the amorphous precursor samples and prevented subsequent sticking at solid state temperatures within the reactor.

TABLE I
Characteristics of PET Precursors Used in Solid State Evaluations

cPrecursor	Goodyear VFR-6014	Firestone A	Eastman 7328
Inherent viscosity (IV)	0.63	0.55	0.57
Molecular weight (M_n)	19,900	16,300	17,200
Monomer used	Terephthalic acid (TPA)	Terephthalic acid (TPA)	Dimethyl terephthalate (DMT)
Catalyst system	Antimony (Sb)	Antimony (Sb)	Antimony–Manganese–Cobalt–Titanium (Sb–Mn–Co–Ti)

Solid State Polymerization

A bench scale reactor, with a 50-g sample capacity, was used to solid state polymerize precursor samples at various time, temperature, and atmospheric conditions. The cylindrical, stainless steel reactor was equipped with a gas inlet situated below the sample chamber, to permit preheated purge gas to pass through the pellet bed during solid stating. The purge gas was used to distribute heat evenly throughout the sample chamber and to remove volatile reaction products from the pellet atmosphere. The purge, controlled at a constant predetermined flow rate, was preheated while passing through a 10 ft × 1/4 in. coil of stainless steel tubing. Thermocouples at three individual locations within the reaction chamber were used to monitor pellet bed temperatures during polymerization.

A fluidized sand bath, produced by Techne Inc. was used to heat the reactor, purge gas, and sample. Sand, fluidized by air, was heated with two electric coils to solid state temperatures, controlled within ±3°F.

The following polymerization steps were followed at various time and temperature conditions for most of the samples evaluated during this study. Samples designated as "wet" were not predried before polymerization, and precautions for removing oxygen from the reaction chamber were omitted for samples solid stated in air.

1. The reactor was filled with predried precursor, closed, and purged with dry nitrogen. Purging was continued until levels of oxygen found in the spent nitrogen purge gas were reduced to less than 0.2%. Oxygen levels were monitored using a Hewlett-Packard gas chromatograph equipped with a thermoconductivity detector and a 20 ft × 1/8 in. stainless steel column packed with 60/80 mesh molecular sieve.

2. Under continued nitrogen purge, at the desired flow rate, the reactor containing oxygen-free, dry precursor was immersed in the constant temperature fluidized sand bath. Thermocouples within the reaction chamber were used to monitor resin temperatures throughout polymerization. It was determined that 0.5 h was required to achieve the desired reaction temperature. Reaction times were measured only after these temperatures had been attained.

3. After each reaction had been completed, the reactor, still under nitrogen purge, was removed from the sand bath and cooled with external air flow. Nitrogen purge was maintained until the resin bed had been cooled to room temperature. Samples were then removed for further analysis.

Inherent Viscosity (IV)

Inherent viscosity determinations were made in 60/40 phenol–tetrachloroethane at 25°C using Cannon-Ubbelohde dilution viscometers. Sample concentrations of 0.25 g/100 mL were used. All samples were dried in a vacuum oven at 150°C prior to viscosity measurements.

Determination of Moisture in PET Pellets

A DuPont solids moisture analyzer (26-321A) was used to measure the moisture content of PET pellets used in these experiments. Samples were heated at 160°C until all moisture had been expelled. The moisture was calculated as:

Percent moisture = $(C_s - C_b)/W_s \times 100$ where C_s = counts obtained for sample (μg), C_b = counts obtained for blank (μg), and W_s = weight of sample (μg). The above procedure yields an accuracy of $\pm 0.001\%$.

Residual Acetaldehyde

Concentrations of residual acetaldehyde present in precursors and resins, as received or after various experimental procedures, were measured using materials ground to 20 mesh. Samples of about 600 mg were weighed into 7 mL venoject tubes, sealed with rubber serum caps, and heated for 30 min at 150°C in an aluminum heating block. After completion of the heating cycle, headspace samples of acetaldehyde were removed and injected into a Perkin-Elmer 900 gas chromatograph, equipped with a flame ionization detector and a 5 ft × 1/8 in. O.D. stainless steel column packed with 80/100 mesh Porapak QS. For calculation, chromatogram peak heights corresponding to acetaldehyde were measured and compared to those of an acetaldehyde standard. Concentration of acetaldehyde was reported as ppm (w/w).

Acetaldehyde Generation

Acetaldehyde generation was monitored using a Chromalytics 1047 concentrator in conjunction with a Perkin-Elmer 900 gas chromatograph. Before analysis, samples were vacuum-dried overnight at 145°C to remove residual acetaldehyde and moisture. During analysis, samples of unground resin weighing 70–90 mg were placed in a predried heating chamber and purged with dry nitrogen to obtain an oxygen-free environment. With continued nitrogen purge, a 285°C cylindrical oven was then placed over the sample chamber and held there for 8 min to facilitate acetaldehyde generation. Generated acetaldehyde was swept with the nitrogen purge into the concentrator U-tube trap packed with 60/80 mesh Tenax GC. After the heating cycle was completed, the trap contents were volatilized and backflushed into the gas chromatograph with its helium carrier gas. Acetaldehyde separation was achieved using a 6 ft × 1/8 in. chromatographic column of 80/100 mesh Porapak QS and quantitatively monitored with a flame ionization detector. Peak size was measured and generated acetaldehyde ppm (w/w) calculated using a previously determined response factor, obtained with an acetaldehyde gas standard.

Carboxyl End Group Determination

Carboxyl end group concentrations were determined for samples dissolved in boiling benzyl alcohol (0.5 g/5 mL) and diluted with chloroform. A 0.1 mL ultramicro buret was used for titration with 0.1*N* sodium hydroxide to the first faint pink color change of Phenol Red indicator. A reagent blank and empirical correction factor were also utilized in the calculation.

Calculation.

$$\text{Carboxyl content (eq/}10^6\text{ g)} = \frac{(\text{net } \mu\text{L NaOH})\,(N \text{ NaOH})}{\text{wt PET (g)}} - C \text{ eq/}10^6 \text{ g}$$

Blank = combined titer value of benzyl alcohol, chloroform, and indicator treated in the same manner as the sample

Net μL NaOH for titration = total titer value for the sample titration minus the blank titer value.

C = correction factor determined as a function of dissolving time and provided in an unpublished Goodyear report

Melting Behavior

Melting behaviors of samples solid stated at various conditions were monitored using a Perkin-Elmer Differential Scanning Calorimeter (DSC-2). Endotherms of ground, dried samples were recorded at heating rates of 10°C/min, under a nitrogen atmosphere.

RESULTS AND DISCUSSION

Kinetics of Polymerization in the Solid State

Inherent viscosity changes were used to monitor the molecular weight increases of PET at various solid state conditions. Vacuum-dried samples were polymerized in a bench scale reactor, under a 1000 cc/min nitrogen purge, for times from 2 through 16 h, at temperatures from 200 through 250°C. As an example of changes obtained during solid stating, Figure 1 shows viscosity as a function of reaction time at a variety of temperature conditions. Similar curves were obtained for the other polyester materials.

The relationship between inherent viscosity (IV) and weight average molecular weight (M_w) is given by[15]

$$\text{IV} = 4.68 \times 10^{-4}(M_w)^{0.68} \tag{1}$$

in (60/40) phenol/tetrachloroethane at 25°C. For PET

$$M_w \approx 2M_n$$

Therefore,

$$\text{IV} = 7.50 \times 10^{-4}(M_n)^{0.68} \tag{2}$$

or

$$M_n = 3.92 \times 10^4(\text{IV})^{1.47} \tag{3}$$

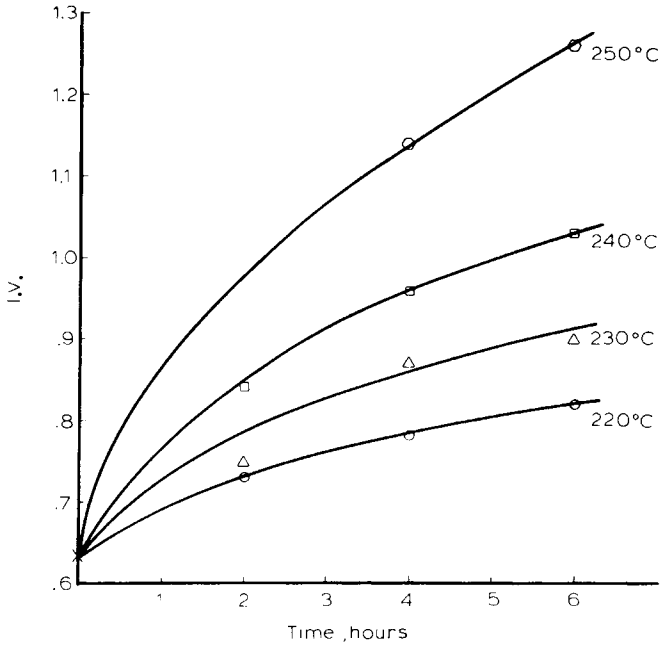

Fig. 1. Inherent viscosity as a function of time at various solid state temperatures. (Nitrogen purge at 1000 cc/min.)

Molecular weights were determined from sample inherent viscosity values, using the relationship shown in eq. (3). Results obtained at each solid state condition are tabulated on Tables II–IV.

Flory[16] has shown degree of polymerization to be approximately proportional to the square root of time for third-order condensation reactions, except during early stages of the reaction. The relationship of molecular weight to the square root of solid state reaction time is shown graphically in Figure 2.

TABLE II
Solid State Behavior of Goodyear VFR-6014 as a Function of Time and Temperature Reaction Conditions

Temperature (°C)	Time (h)	Inherent viscosity	Molecular weight
As received	0	0.63	1.99×12^4
220	2	0.73	2.47×10^4
220	4	0.78	2.72×10^4
220	6	0.82	2.93×10^4
230	2	0.75	2.57×10^4
230	4	0.87	3.19×10^4
230	6	0.90	3.36×10^4
240	2	0.84	3.03×10^4
240	4	0.96	3.69×10^4
240	6	1.03	4.09×10^4
250	4	1.14	4.75×10^4
250	6	1.26	5.51×10^4

TABLE III
Solid State Behavior of Firestone A as a Function of Time and Temperature Reaction Conditions

Temperature (°C)	Time (h)	Inherent viscosity	Molecular weight
As received	0	0.55	1.63×10^4
200	4	0.60	1.85×10^4
200	6	0.63	1.99×10^4
220	2	0.63	1.99×10^4
220	4	0.74	2.52×10^4
220	6	0.72	2.42×10^4
230	2	0.67	2.18×10^4
230	4	0.75	2.57×10^4
230	6	0.92	3.47×10^4
240	2	0.78	2.72×10^4
240	4	0.95	3.64×10^4
240	6	0.99	3.86×10^4
250	2	0.84	3.03×10^4

TABLE IV
Solid State Behavior of Eastman 7328 as a Function of Time and Temperature Reaction Conditions

Temperature (°C)	Time (h)	Inherent viscosity	Molecular weight
As received	0	0.57	1.72×10^4
200	16	0.69	2.25×10^4
220	2	0.67	2.18×10^4
220	4	0.69	2.27×10^4
220	6	0.73	2.47×10^4
220	16	0.85	3.09×10^4
230	2	0.70	2.32×10^4
230	4	0.74	2.52×10^4
230	6	0.79	2.77×10^4
230	16	0.93	3.52×10^4
240	2	0.76	2.62×10^4
240	4	0.82	2.93×10^4
240	6	0.85	3.09×10^4
250	2	0.83	2.98×10^4
250	4	0.88	3.25×10^4
250	6	0.92	3.47×10^4

These data represent the reaction of Goodyear precursor at various temperatures and illustrate the behavior of all three experimental materials. Dröscher and Wegner[17] have plotted similar data to obtain linear relationships between molecular weight and the square root of reaction time. Their data also show increased slope at higher solid state temperatures. They found these relationships to hold for times up to 16 h from 219 to 254°C. At very long times, degradation effects produce deviations from linearity of the relationships.

As can be seen in Figure 2, lines extended from initial precursor molecular weight, through values obtained after solid stating for various times at each

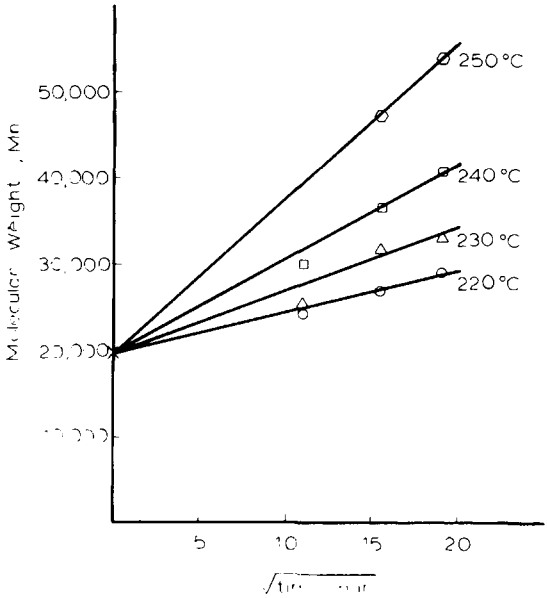

Fig. 2. Molecular weight as a function of the square root of time at various solid state temperature. (Nitrogen purge at 1000 cc/min.)

temperature, are described by the following empirical equation:

$$M_n = M_{n0} + k\sqrt{t} \tag{4}$$

which can be solved to give the equilibrium rate constant (k) for solid state polymerization at each condition:

$$k = \frac{M_n - M_{n0}}{\sqrt{t}} \tag{5}$$

where M_n = number average molecular weight at time t, M_{n0} = initial number average molecular weight of precursor, and t = time (min) of solid state reaction at each temperature.

At each solid state temperature, an average value for k is obtained. The natural log of this value ($\ln k$) can be plotted versus $1/T$ (K) to obtain an Arrhenius plot as shown in Figure 3. Values for activation energy (ΔE) and frequency factor (A) may be calculated from this plot or using an exponential regression program:

$$k = Ae^{-\Delta E/RT} \tag{6}$$

where A = collision, frequency factor for propagation, ΔE = energy of activation for propagation cal/mol, R = gas constant, 1.987 cal/mol K, and T = temperature (K).

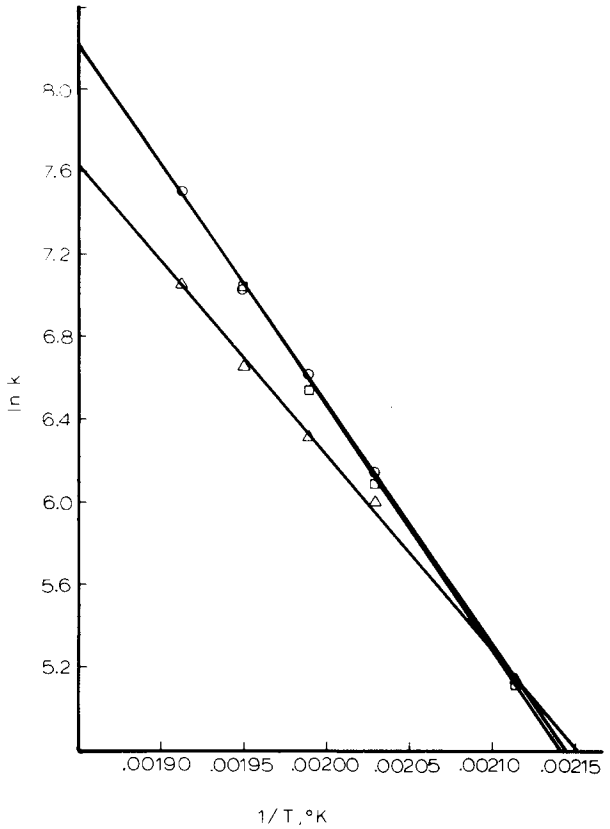

Fig. 3. Arrhenius plot of rate constants for molecular weight increases of three PET materials at various solid state temperatures: (○) Goodyear; (□) Firestone; (△) Eastman.

Combining eqs. (5) and (6), one obtains

$$\frac{M_n - M_{n0}}{\sqrt{t}} = Ae^{-\Delta E/RT} \tag{7}$$

which can be rearranged to give

$$M_n = M_{n0} + Ae^{-\Delta E/RT}\sqrt{t} \tag{8}$$

This kinetic rate equation describes the empirical relationship of solid state time, temperature, and polymer molecular weight. With values for ΔE and A substituted, the following equations were obtained for precursors evaluated in this study:

Goodyear 6014.

$$M_n = 1.99 \times 10^4 + 624 \times 10^{10} e^{-22{,}800/1.987T}\sqrt{t}$$

Firestone A.

$$M_n = 1.63 \times 10^4 + 828 \times 10^{10} e^{-23{,}200/1.987T}\sqrt{t}$$

Eastman 7328.

$$M_n = 1.72 \times 10^4 + 5.70 \times 10^{10} e^{-18,400/1.987T} \sqrt{t}$$

As can be seen, values calculated for activation energy and frequency factor are very similar for Goodyear and Firestone materials. Both of these precursors were produced using terephthalic acid monomer and antimony catalyst systems. Eastman values for activation energy and frequency factor are lower than those of the other two materials, indicating greater ease of polymerization and less frequency of interaction. The Eastman precursor was produced using dimethyl terephthalate monomer. Its catalyst system contained manganese and cobalt as transesterification catalysts with antimony and titanium for polycondensation. These results are in agreement with work reported by Zimmermann and co-workers[7-11] showing that samples prepared with manganese and cobalt catalyst systems polymerize more readily than those containing just antimony catalysts.

Moisture Effects

The effects of solid stating undried PET precursor have been investigated in terms of inherent viscosity changes resulting from various exposure conditions. Initial experiments were conducted with small (~ 1 g) samples heated in a DuPont Thermogravimetric Analyzer (TGA) oven for times up to 60 min. Samples had moisture concentrations of 0.24% prior to solid stating and were permitted to dry during heating. A dry nitrogen purge (~ 40 cc/min) was used to prevent oxidative degradation and remove volatile reaction products. The TGA system was chosen for this portion of the study because it provided better short time temperature control than the bench scale reactor.

Table V shows results obtained at a variety of time and temperature exposure conditions. This data is exhibited graphically in Figure 4. The upper drawing shows sample inherent viscosity (IV) plotted as a function of reaction temperature, after 15 min of exposure. As can be seen at temperatures up to 200°C, no IV loss was measured. Losses noted at 210 and 220°C increase with exposure to higher temperatures. The lower drawing illustrates the effects of increased exposure time at 220°C. At this temperature the material begins to degrade immediately upon thermal exposure, obtaining its lowest value after ~ 15 min. With longer exposure time IV increases, indicating polymerization

TABLE V
Inherent Viscosity as a Function of Reaction Time and Temperature for "Wet" PET, Solid Stated without Drying

cTemp (°C)	IV of PET after various heating times				
	0 min	8 min	15 min	30 min	60 min
Control	0.63	—	—	—	—
175	—	—	0.62	—	—
200	—	—	0.62	—	—
210	—	—	0.58	—	—
220	—	0.60	0.54	0.60	0.64

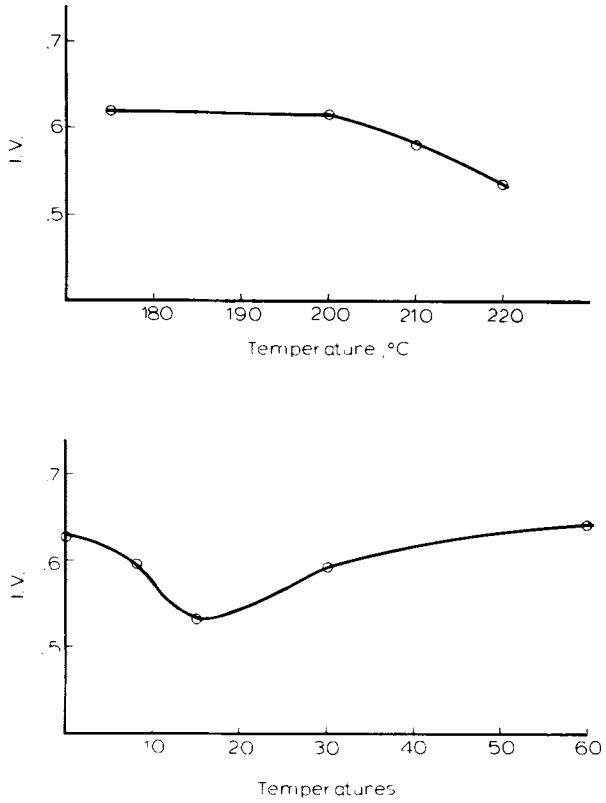

Fig. 4. Inherent viscosity changes as a function of temperature and time for PET samples solid stated "wet," without drying.

is occurring more rapidly than hydrolytic degradation, as sample moisture levels are reduced by drying at solid state conditions.

Additional experiments were conducted using the bench scale reactor and precursor with an initial moisture concentration of 0.45%. Results of this work are shown in Table VI. It will be noted that IV values show smaller decreases after exposure to bench scale vs. TGA heating conditions. This is because bench scale samples do not achieve thermal equilibrium until about 30 min after being placed in the constant temperature sand bath. Because of the increased time required to reach solid state temperatures, bench scale samples (with higher moisture concentrations) are partially dried before temperatures are high enough to cause hydrolytic degradation.

Table VI shows total heating times which are counted from when the reactor is placed in the sand bath, as well as heating times after equilibrium conditions have been reached. Table VII shows moisture concentrations measured at the upper and lower portion of the reactor after various total elapsed immersion times. Actual thermocouple temperatures, recorded at these times, are shown in parenthesis beside each moisture concentration. Only lower reactor samples have been used for IV determinations. It can be seen that these samples are fairly dry (after ~ 15 min), before thermal equilibrium has been achieved. Rate constants were calculated using this data

TABLE VI
Solid State Behavior of "Wet" Goodyear VFR-6014 as a Function of Time and Temperature Reaction Conditions

Temperature (°C)	Total heating time (min)	Time after temperature reached (min)	Inherent viscosity	Molecular weight
As received	0	—	0.63	1.99×10^4
200	15	—	0.60	1.86×10^4
200	30	—	0.60	1.84×10^4
200	60	30	0.61	1.89×10^4
200	120	90	0.63	1.98×10^4
220	15	—	0.59	1.81×10^4
220	30	—	0.59	1.81×10^4
220	60	30	0.63	1.97×10^4
220	120	90	0.65	2.10×10^4
220	150	120	0.68	2.23×10^4
220	270	240	0.75	2.56×10^4
220	330	300	0.78	2.72×10^4
240	15	—	0.59	1.79×10^4
240	30	—	0.62	1.93×10^4
240	60	30	0.68	2.22×10^4
240	120	90	0.78	2.70×10^4
240	270	240	0.95	3.62×10^4

as had been done for previous dry samples. If initial molecular weight values were taken as the lowest molecular weight measured during the initial stages of the reaction; rate of polymerization was found to be similar to that calculated for dry material. For wet resins $A = 489 \times 10^{10}$ and $\Delta E = 22.6$ kcal/mol vs. $A = 624 \times 10^{10}$ and $\Delta E = 22.8$ kcal/mol for dry resin. Additional reaction time, however, must be allowed to permit repolymerization to make up for IV loss which occurs during hydrolytic degradation. The effects of hydrolytic degradation have not yet been investigated in terms of degradation products, thermal and oxidative stability, or material performance.

TABLE VII
Moisture Concentration Remaining in Resin within Reactor after Various Immersion Times in Constant Temperature Sand Bath

Temperature of sand bath (°C)	Total immersion time (min)	% Moisture remaining in resin: Upper portion of reactor	Lower portion of reactor
200	15	0.07 (173)[a]	0.008 (195)[a]
200	30	0.01 (185)[a]	0.006 (198)[a]
200	60	0.002 (200)[a]	— (200)[a]
220	15	0.03 (200)[a]	0.006 (218)[a]
220	30	0.006 (217)[a]	0.001 (220)[a]
220	60	0.004 (220)[a]	0.001 (220)[a]
240	15	0.02 (210)[a]	0.005 (233)[a]
240	30	0.004 (227)[a]	— (240)[a]
240	60	0.001 (240)[a]	— (240)[a]

[a] Resin temp (°C).

TABLE VIII
Residual Acetaldehyde and 2-Methyl Dioxolane Present in Goodyear VFR-6014, as a Function of Solid State Time and Temperature Conditions

Temperature (°C)	Time (h)	Residual [ppm (w/w)]	
		Acetaldehyde	2-Methyl dioxolane
As received	—	24	1.0
150	1.5	16	0.7
150	2.0	14	0.7
150	2.0	15	0.7
150	2.5	12	0.7
150	4.5	7.7	0.5
150	6.0	7.8	0.7
150	18.0	2.1	0.5
180	2.0	5.6	0.5
180	4.0	3.3	0.4
180	6.0	2.4	0.4
200	1.0	5.2	0.5
200	2.0	3.6	0.5
200	3.0	3.4	0.6
200	4.0	2.9	0.4
200	6.0	2.0	0.3

Residual Acetaldehyde and 2-Methyl Dioxolane

The effects of solid state temperatures on residual acetaldehyde and 2-methyl dioxolane concentrations were monitored. Precursor samples were placed in the bench scale reactor as received, because drying would have removed the residuals. A constant nitrogen purge at 1000 cc/min was used to prevent oxidative degradation during heating. Temperatures of 200°C and below were utilized to minimize hydrolytic degradation and polymerization which would have generated additional acetaldehyde. The generated acetaldehyde would have been indistinguishable from the residual. Results of this evaluation are shown on Table VIII. Concentrations of 2-methyl dioxolane were reduced to about half of their original values. Removal of residual acetaldehyde is shown graphically in Figure 5. It can be seen that increased reactor temperatures significantly reduce the times required to acheive low concentrations of residual acetaldehyde, although low levels can also be reached after long reaction times at lower temperatures.

Acetaldehyde Generation at Melting Conditions

When PET is held at melting conditions, it is known to degrade, generating acetaldehyde as one of its major volatile decomposition products. For this reason acetaldehyde generation has been used to indicate the thermal stability of various PET materials after polymerization at each solid state condition. Results can be seen on Table IX. The lowest generation values at melting conditions are seen for samples exposed to long time and/or high temperature solid state conditions. Inherent viscosity is seen to increase under these conditions; however, it appears to be unrelated to acetaldehyde generation. For example, samples with similar IVs show different generation values. It has also been noted, that minimal generation values are different for each resin

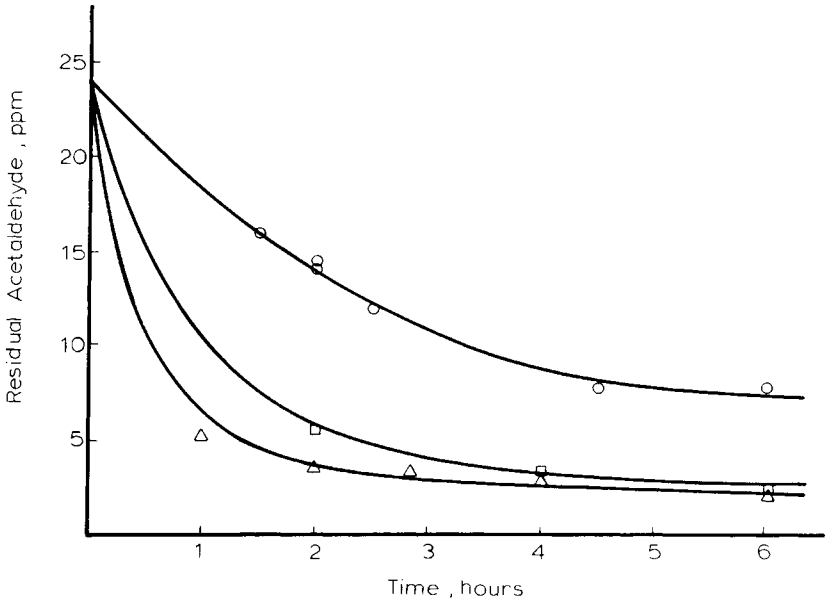

Fig. 5. Residual acetaldehyde concentration as a function of reaction time at various solid state temperatures (°C): (○) 150; (□) 180; (△) 200.

type. Figure 6 shows acetaldehyde generation values for the three resin types after solid state polymerization at various temperatures for 4 h under a 1000 cc/min nitrogen purge. As can be seen, the Eastman material generates higher amounts of acetaldehyde than the other two resins, regardless of solid state conditions. The Eastman resin was prepared from dimethyl terephthalate using a catalyst system containing antimony, manganese, cobalt, and titanium. The other two resins were prepared from terephthalic acid using antimony catalyst systems. The Firestone material shows the least acetaldehyde generation after solid stating at all conditions. After longer time or high temperature solid stating, Goodyear generation values are reduced to those achieved with Firestone. These results are in agreement with those of Zimmermann and co-workers[7-11] and indicate that resins prepared from terephthalic acid using antimony catalyst systems show less degradation during melting than those prepared using dimethyl terephthalate and catalyst systems containing manganese and cobalt.

Air vs. Nitrogen Solid Stating

Additional solid state experiments were done using slightly different experimental conditions. Goodyear VFR-6014 was polymerized with purge flow rates of 500 cc/min, rather than the 1000 cc/min rates previously described. For these experiments, purge atmospheres of air as well as nitrogen were used in order to monitor the effects of reaction environment upon changes in inherent viscosity, acetaldehyde generation, and carboxyl end group concentration.

Results, which are shown in Table X indicate that at 200°C air vs. nitrogen purge has very little effect on inherent viscosity changes. At 210°C, however, resins solid stated in air show significantly less gain in inherent viscosity than

TABLE IX
Acetaldehyde Generation at Melting Conditions and Inherent Viscosity Values, as a Function of Solid State Time and Temperature, for Three PET Materials

Material	Temp (°C)	200		220		230		240		250	
	Time (H)	AA [ppm (w/w)]	IV	AA [ppm (w/w)]	IV	AA [ppm (w/w)]	IV	AA [ppm (w/w)]	IV	AA [ppm (w/w)]	IV
Goodyear	2	—	—	6.9	0.73	6.4	0.75	6.9	0.84	5.6	—
VFR-6014	4	—	—	7.9	0.78	6.6	0.87	5.7	0.96	4.8	1.14
	6	—	—	4.2	0.82	4.1	0.90	4.7	1.03	3.9	1.26
Firestone A	2	—	—	4.4	0.63	4.3	0.67	3.9	0.78	4.1	0.84
	4	6.2	0.60	4.8	0.74	4.5	0.75	4.0	0.95	—	—
	6	5.0	0.63	4.2	0.72	4.4	0.92	3.8	0.99	—	—
Eastman	2	—	—	14.2	0.67	12.2	0.70	14.1	0.76	10.2	0.83
7328	4	—	—	11.5	0.69	11.1	0.74	10.9	0.82	9.5	0.88
	6	—	—	13.1	0.73	11.9	0.79	11.0	0.85	11.0	0.92
	16	11.4	0.69	13.1	0.85	12.9	0.93	—	—	—	—

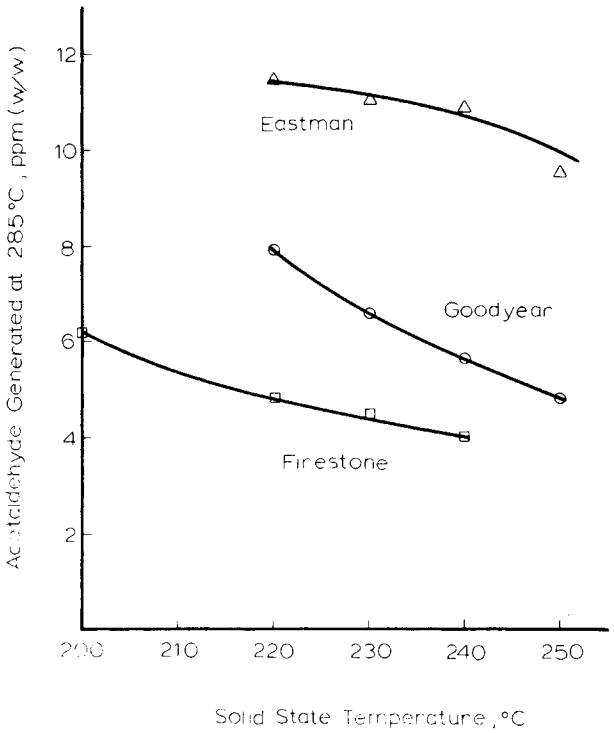

Fig. 6. Acetaldehyde generated at melting conditions as a function of solid state temperature for three PET materials.

equivalent resins solid stated in nitrogen. These results indicate that at higher temperatures in the presence of oxygen, degradation offsets the polymerization of PET. Previously described experiments, as well as this nitrogen solid state data, show that increased polymerization temperature, in an oxygen-free environment, results in an increased rate of molecular weight gain.

Acetaldehyde generation results, shown in Table X and in Figure 7, appear to be superior for air solid stated samples, since less acetaldehyde is generated

TABLE X
Acetaldehyde Generated at Melting Conditions, Carboxyl End Group Concentration, and Inherent Viscosity Values of Goodyear VFR-6014 as a Function of Solid State Time and Temperature in Nitrogen and Air Environments

Temperature (°C)	Time (h)	Environment	AA generated [ppm (w/w)]	—COOH (eq/10^6 g)	IV
200	4	N_2	9.2	30	0.69
200	8	N_2	8.2	26	0.73
210	4	N_2	7.1	27	0.73
210	8	N_2	6.6	26	0.80
220	4	N_2	5.1	—	0.80
230	4	N_2	3.2	—	0.83
200	4	Air	3.6	34	0.71
200	6	Air	4.7	—	0.73
200	8	Air	3.5	39	0.74
210	4	Air	3.5	44	0.69
210	8	Air	2.8	58	0.65

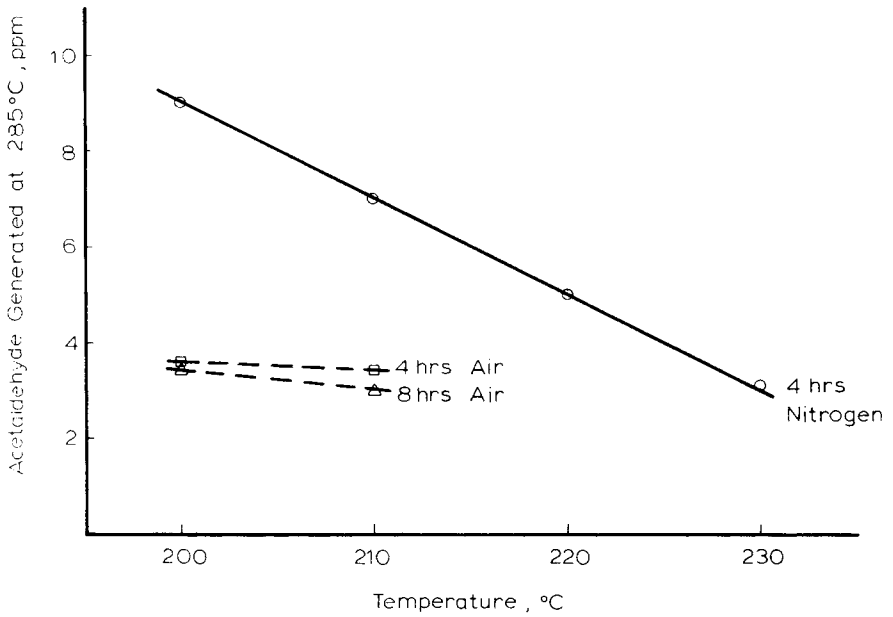

Fig. 7. Acetaldehyde generated at melting conditions as a function of reaction temperature for samples solid stated in air or nitrogen.

during melting of equivalent samples. These results are misleading because, although low amounts of acetaldehyde are generated, degradation has proceeded by another path. During melting, samples solid stated in air showed very poor color stability, developing a yellow color even after 1 min of melting time. Increased intensity of this color was found to correlate with higher temperatures and longer times of air solid stating. Samples solid stated in nitrogen did not exhibit yellowness even after 60 min of melting at 285°C. It must also be noted that, during melting of air solid stated resin, volatile low molecular weight degradation products in addition to acetaldehyde are observed.

Samples solid stated in nitrogen also show low acetaldehyde generation values, if polymerization is conducted at higher temperatures or for longer times. In these cases additional degradation products are not present, samples do not yellow when melted, and inherent viscosity increases are significant.

Changes in carboxyl end group concentration illustrate very well the degradation effects of air solid stating, as can be seen in Figure 8. After air solid stating, particularity at higher temperatures, carboxyl end group concentrations increase significantly. After nitrogen solid stating, carboxyl end group concentrations decrease slightly as would be expected during PET polymerization.

Melting Behavior

Melting behavior observed for PET resin has been found to be directly related to solid state conditions. Differential scanning calorimetry endotherms, obtained at heating rates of 10°C/min for samples solid stated at various temperatures, are shown in Figure 9. These transition temperatures

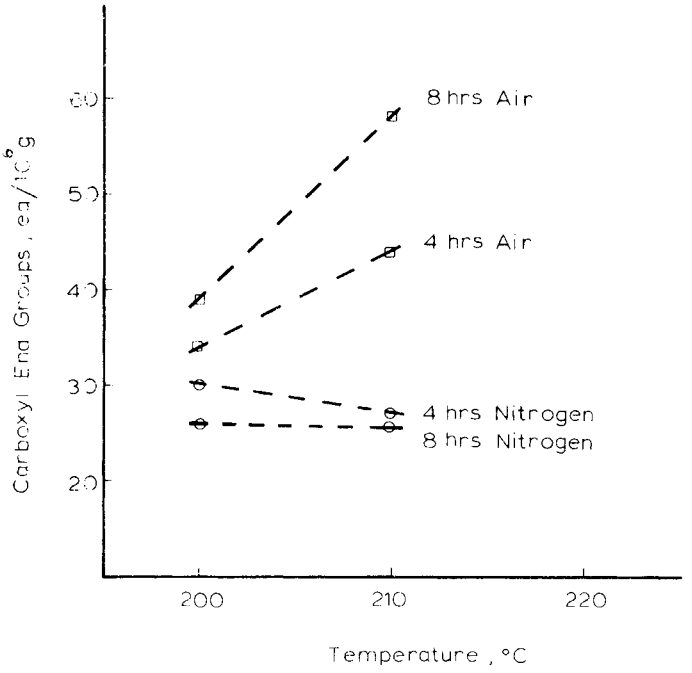

Fig. 8. Carboxyl end group concentration as a function of reaction temperature for samples solid stated in air or nitrogen.

are tabulated in Table XI showing temperatures of initial, peak, and final melting. Similar multiple melting endotherms have been observed by others[18-20] and interpreted on the basis of distributions of crystallite sizes or perfections induced by thermal treatments. As can be seen, at higher solid state temperatures, less temperature difference occurs between the first melting peak (T_{p_1}) and second melting peak (T_{p_2}). Figure 10 shows graphically the relationship $T_{p_2} - T_{p_1} = T$ as a function of solid state temperature. It can also be noted that, as the solid state polymerization temperature is increased, smaller temperature differences occur between reaction temperature and the first melting temperature.

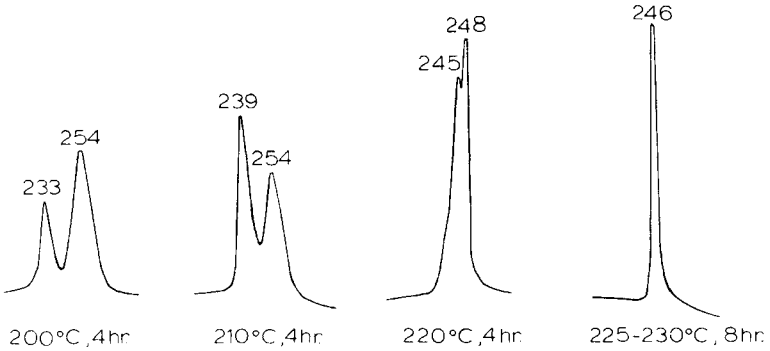

Fig. 9. Differential scanning calorimetry endotherms for samples solid stated at various temperatures.

TABLE XI
Differential Scanning Calorimetry Endotherm Transition Temperatures for Goodyear VFR-6014 as a Function of Solid State Conditions

Solid State Condition		Melting temperatures (°C)			
Temperature	Time (h)	T_i	T_{p_1}	T_{p_2}	T_f
200	4	213	233	254	265
210	4	220	239	254	270
220	4	213	245	248	268
225–230	8	226	246		266

Nitrogen Flow Rate

Acetaldehyde generation at melting conditions has been evaluated in relationship to nitrogen flow rate during solid stating. Results obtained for samples solid stated 4 h at temperatures from 210 to 240°C are shown in Table XII. Samples shown with zero flow rates were solid stated in a vacuum oven and those with medium flow rate in a modified thermogravimetric analysis furnace. Other samples were solid stated in a bench scale reactor, as previously described. Results are illustrated graphically in Figure 11, with acetaldehyde generation plotted as a function of nitrogen flow rate. As can be seen, samples solid stated at equivalent time and temperature conditions generated less acetaldehyde at melting conditions, if they had been exposed to increased nitrogen flow during solid state polymerization.

SUMMARY AND CONCLUSIONS

1. During solid state polymerization of PET, increased time and temperature exposure result in molecular weight gains described by the following equation:

$$M_n = M_{n0} + Ae^{-\Delta E/RT}\sqrt{t}$$

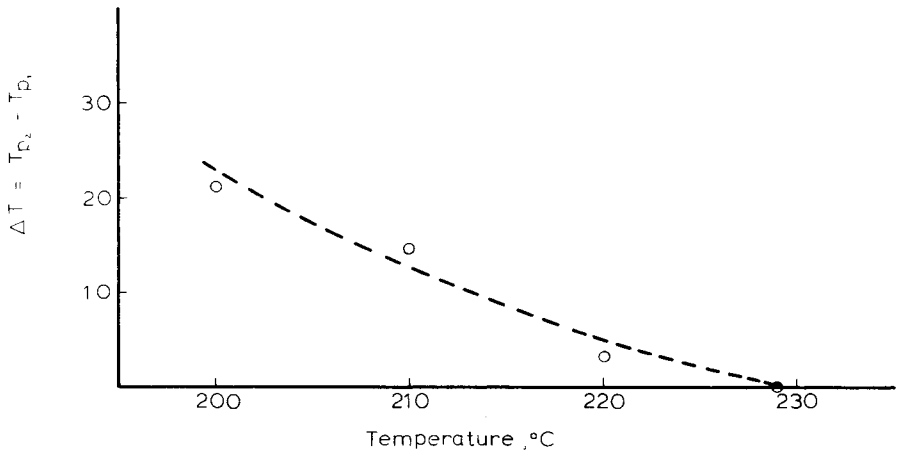

Fig. 10. Relationship of endothermic peak temperature changes ($T_{p_2} - T_{p_1} = \Delta T$) to solid state temperature.

TABLE XII
Acetaldehyde Generation at Melting Conditions and Inherent Viscosity Values for Goodyear VFR-6014 Solid Stated 4 h at Various Temperatures as a Function of Nitrogen Flow Rate

Linear flow rate, (ft/s)	Temperature (°C)	AA generated [ppm (w/w)]	IV
0	210	10	0.69
0	220	9.5	0.72
0	230	8	0.79
0	240	8	0.93
0.005	210	9	0.78
0.005	220	7	0.83
0.005	230	5	0.87
0.005	240	4	0.89
0.05	200	9	0.69
0.05	210	7	0.73
0.05	220	5	0.80
0.05	230	3.2	0.83
0.05	240	1.4	—

Values for activation energy (ΔE) and frequency factor (A) are dependent upon catalyst and monomer systems used during precursor polymerization.

2. Hydrolytic degradation causes initial reductions of molecular weight if precursors are solid stated without being dried. With increased exposure to solid state conditions, however, the hydrolytically degraded resin dries and repolymerizes at rates similar to those observed for resins that have not undergone hydrolysis.

3. Levels of residual acetaldehyde and 2-methyl dioxolane are reduced by increased reactor time and temperature conditions. Higher temperatures significantly reduce times required to achieve low concentrations of residuals.

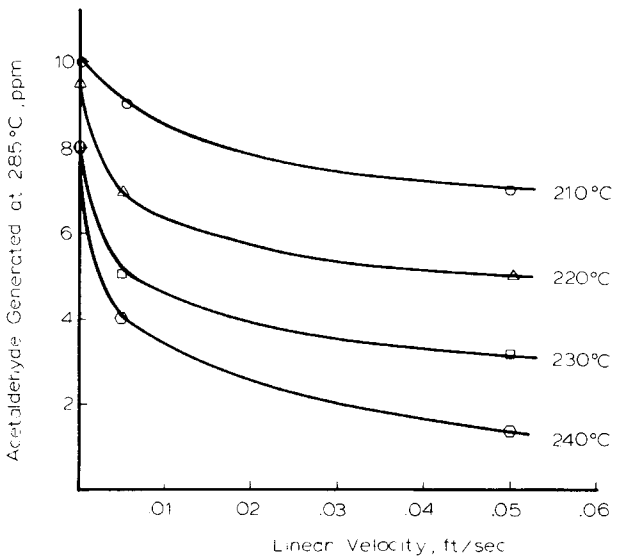

Fig. 11. Acetaldehyde generation at melting conditions, as a function of nitrogen flow rate, at various solid state temperatures (Goodyear VFR-6014).

4. Acetaldehyde generation at melting conditions is apparently unrelated to molecular weight. Resin prepared with DMT monomer and a catalyst system containing manganese and cobalt degrades more readily (generates more acetaldhyde) during melting than resins prepared with TPA monomer and antimony catalyst. Longer times and higher temperatures of solid stating reduce acetaldehyde generation values for all samples.

5. Exposure to oxygen during solid stating has little effect on molecular weight if temperatures are maintained below 200°C. At 210°C and above, degradation offsets polymerization, resulting in reduced or negative gains in molecular weight. During melting, less acetaldehyde is generated by samples solid stated in air; however, degradation proceeds by a different path, giving other volatile degradation products and poor color stability. After increased time and temperature exposure under nitrogen, samples maintain color stability while showing reduced acetaldehyde generation and higher molecular weights. Carboxyl end group concentrations, increase significantly after air solid stating at higher temperatures. After nitrogen solid stating, concentrations are reduced as would be expected during PET polymerization.

6. At higher solid state temperatures, the temperature difference between the first and second melting peak is reduced, as is the difference between these peak temperatures and the solid state temperature.

7. Samples solid stated at èquivalent time and temperature conditions generate less acetaldehyde if exposed to increased nitrogen purge flow rate during polymerization.

References

1. I. Marshall and A. Todd, *Trans. Faraday Soc.*, **49**, 67–78 (1953).
2. E. P. Gooding, *Thermal Degradation of Polymers*, Society of Chemical Industry Monograph #13, 1961.
3. I. E. Kardash, A. N. Prarednikov, and S. S. Medvedev, *Dokl. Akad. Nauk USSR*, **156**, 658 (1964).
4. K. Tomita, *Polymer*, **17**, 221 (1976).
5. C. M. Fontana, *J. Polym. Sci.*, **6**, 2343–2358 (1968).
6. S. Chang, M. Sheu, and N. Chang, *J. Polym. Sci.*, **20**, 2053–2061 (1982).
7. H. Zimmermann and N. T. Kim, *Polym. Eng. Sci.*, **20**, 680 (1980).
8. H. Zimmermann, *Developments in Polymer Degradation*, Applied Science, London, 1984, Vol. 5, Chap. 3.
9. H. Zimmermann, D. Becker, and E. Schaaf, *J. Appl. Polym. Sci., Appl. Polym. Symp.*, **35**, 183–191 (1979).
10. H. Zimmermann and D. Chu, *Faserforsch. Textiltech.*, **24**, 445–452 (1973).
11. H. Zimmermann and D. Becker, *Faserforsch. Textiltech.*, **24**, 479–483 (1973).
12. D. A. S. Ravens and I. M. Ward, *Trans. Faraday Soc.*, **57**, 150 (1961).
13. W. McMahon, H. A. Birdsall, G. R. Johnson, and C. T. Camilli, *J. Chem. Eng. Data*, **4**, 57–79 (1959).
14. S. A. Jabarin and E. A. Lofgren, *Polym. Eng. Sci.*, **24** (13), 1056–1063 (1984).
15. P. D. Richie, *Society of Chemical Industry Monogr.*, **13**, 107 (1961).
16. P. Flory, *Principles of Polymer Chemistry*, Cornell Univ. Press, Ithaca, NY, 1953, Chap. III.
17. M. Dröscher and G. Wegner, *Polymer*, **19**, 43–47 (1978).
18. R. C. Roberts, *Polymer*, **10**, 117 (1969).
19. E. L. Lawton and D. M. Cates, *Polym Prepr.*, **9** (1), 851 (1968).
20. F. Fontaine, J. Ledent, G. Groeninckx, and H. Reynaers, *Polymer*, **23**, 185 (1982).

Received December 31, 1985
Accepted March 18, 1986